The Egyptian Journal of Remote Sensing and Space Sciences (2013) **16**, 17–21

National Authority for Remote Sensing and Space Sciences

The Egyptian Journal of Remote Sensing and Space Sciences

www.elsevier.com/locate/ejrs
www.sciencedirect.com

RESEARCH PAPER

Distribution of thermodynamic variables inside extra-solar protoplanets formed via disk instability

G.C. Paul *, S.K. Bhattacharjee

Department of Mathematics, University of Rajshahi, Rajshahi 6205, Bangladesh

Received 4 August 2012; accepted 29 November 2012
Available online 3 January 2013

KEYWORDS
Conductive–radiative;
Disk instability;
Jupiter;
Protoplanet;
Thermodynamic variables

Abstract In this paper, distribution of thermodynamic variables inside extra-solar protoplanets in their initial stages, formed by gravitational instability, is presented. The case of conduction–radiation is considered regarding the transference of heat inside the protoplanets. The results are found to compare well with the ones obtained by other investigations.

1. Introduction

Both core accretion and disk instability advocated in the past can, in principle, form gas giant protoplanets. In the core accretion model, the heavy element core is formed by the accretion of planetesimals from the disk followed by further accretion of the surrounding gas (Pollack et al., 1996; Hubickyj et al., 2005). This mechanism has been adopted as the main theory of planetary formation both in our solar system and elsewhere. With the difficulties encountered with the core accretion models, the alternative theory with disk instability and the gravitational collapse of an unsegregated protoplanet which was in vogue in the 1970s when a great deal of now forgotten work was carried out has been reformulated with fragmentation from massive protoplanetary disks and has been advanced through the work of many authors (see e.g., Cha and Nayakshin, 2011; Nayakshin, 2010; Boley et al., 2010). Though some investigations argued that disk instabilities are unable to lead to the formation of self-gravitating, dense clumps (e.g., Pickett et al., 2000; Cai et al., 2006a,b; Boley et al., 2007a,b), the idea is believed to be the promising route for the rapid formation of giant planets in our solar system and elsewhere. Despite substantial study and progress in recent decades, the initial structures of isolated gaseous giant protoplanets formed via disk instability are still unknown and different models predict different initial characteristics (Helled and Schubert, 2008). As for example, the investigation of Nayakshin (2010) predicted colder protoplanets than the ones found in Helled and Schubert (2008) and Mayer et al. (2002, 2004) predicted denser and hotter protoplanets than the ones predicted by Boss (1997, 2007). Boss (1997) in his simulation assumed an initial protoplanet to be fully radiative, Helled and Schubert (2008) found such protoplanets to be fully convective with a thin outer radiative zone, while Paul et al. (2012) and Senthilkumar and Paul (2012) investigated the initial configurations of protoplanets assuming them to be fully convective.

In this paper we intend to determine the internal configuration of protoplanets formed by disk instability assuming the

* Corresponding author. Tel.: +88 0721 711108; fax: +88 0721 750064.
E-mail addresses: pcgour2001@yahoo.com (G.C. Paul), skbru@yahoo.com (S.K. Bhattacharjee).
Peer review under responsibility of National Authority for Remote Sensing and Space Sciences.

ELSEVIER Production and hosting by Elsevier

1110-9823 © 2012 National Authority for Remote Sensing and Space Sciences. Production and hosting by Elsevier B.V. All rights reserved.
http://dx.doi.org/10.1016/j.ejrs.2012.11.004

mode of transference of heat inside to be conductive-radiative and intend to show how they compare the results obtained through different approaches.

The rest of the paper is organized as follows. Section 2 deals with theoretical foundation of the problem. A detailed procedure of numerical approach for the solution is presented in Section 3. Result, discussion and conclusion are given in Section 4.

2. Theoretical foundation

2.1. Energy balance

Our model assumes a non-rotating, non-magnetic spherical giant gaseous object of solar composition in the mass range 0.3–10 M_J, where M_J is the mass of Jupiter. The choice of the mass range is because it covers most of the observed mass range of extrasolar giant planets (see, e.g., Helled and Schubert, 2008). The object is assumed to be in a steady state of quasi-static equilibrium in which the ideal gas law holds well. For heat transfer inside such an object, we consider the conductive–radiative case. We follow Bohm-Vitense (1997) for heat flux in the conductive–radiative heat transport in which the formulation states that the total heat flux in which both conduction and radiation play their role in transference of heat being given by

$$F(r) = 4\pi r^2\left(-\frac{16}{3K}\sigma T^3\frac{dT}{dr}\right) \tag{1}$$

$$\text{with}\quad \frac{1}{K} = \frac{1}{K_{cm}} + \frac{1}{K_{hc}}, \tag{2}$$

where σ is the Stefan–Boltzmann constant and η is the thermal conductivity of the gas and K_{cm} and $K_{hc} = 16\sigma T^3/(3\eta)$ are the radiative and conductive absorption coefficients respectively.

In a protoplanet, the source of energy being gravitational, some energy will be released due to its quasi-static contraction. Half of this released energy is used to raise the internal temperature and the other half goes through radiation. However, the system is in a steady state, so no heat will go into raising the temperature. Therefore, all the energy released will be available for energy flux. If we consider a spherical surface of radius r inside a protoplanet of radius R, the amount of energy available as the heat flux through the sphere of radius r is given by

$$F(r) = -\frac{dE(r)}{dt}, \tag{3}$$

where $E(r)$ is the total energy of the system of radius r and is given by

$E(r) = -\tau\frac{GM^2(r)}{r}$, where τ is a constant of order unity whose value depends on the internal structure of the system, G is the universal gravitational constant and $M(r)$ is the mass interior to a radius r.

Since $M(r)$ remains constant during contraction, therefore, with $E(r)$ Eq. (3) can be written as

$$F(r) = \tau\frac{GM^2(r)}{r^2}\frac{dr}{dt}. \tag{4}$$

For uniform contraction the Eq. (4) can be written as (see Paul et al., 2008)

$$F(r) = \frac{C_R}{R}\frac{GM^2(r)}{r}, \tag{5}$$

where C_R is an unknown constant. We shall consider this constant as a free parameter.

From Eqs. (1 and 5) with the help of Eq. (2), we get

$$-\frac{16}{3}\sigma\, T^3\frac{dT}{dR}\left(\frac{1}{K_{cm}} + \frac{1}{K_{hc}}\right) = \frac{C_R}{4\pi R}\frac{GM^2(r)}{r^3}.$$

Substituting for K_{hc}, we have

$$\left(\frac{16\sigma\, T^3(r)}{3K_{cm}} + \eta\right)\frac{dT(r)}{dr} = -C_R\frac{GM^2(r)}{4\pi R r^3}. \tag{6}$$

But $K_{cm} = nK_{at}$ (Bohm-Vitense, 1997), where n is the number of particles per unit volume and K_{at} is the absorption cross section of each particle. It is found that K_{at} is roughly equal to 2×10^{-24} cm^2 (Bohm-Vitense, 1997). With this value K_{cm} becomes

$$K_{cm} \approx \frac{2\times10^{-24}\rho(r)}{H},$$

where H is the mass of a hydrogen atom.

Substituting this value of K_{cm} in Eq. (6), we have the conductive–radiative flux in the form

$$\left(\frac{8\sigma H}{3\times10^{-24}}\frac{T^3(r)}{\rho(r)} + \eta\right)\frac{dT(r)}{dr} = -\frac{C_R}{4\pi R}\frac{GM^2(r)}{r^3}. \tag{7}$$

2.2. Protoplanetary structure

If the energy equation is given by (7), then the structure of the protoplanets can be given by the following set of equations:

The equation of hydrostatic equilibrium,

$$\frac{dP(r)}{dr} = -\frac{GM(r)}{r^2}\rho(r). \tag{8}$$

The equation of conservation of mass,

$$\frac{dM(r)}{dr} = 4\pi r^2\rho(r). \tag{9}$$

The equation of conductive–radiative heat flux,

$$\left(\frac{8\sigma H}{3\times10^{-24}}\frac{T^3\ (r)}{\rho(r)} + \eta\right)\frac{dT(r)}{dr} = -\frac{C_R}{4\pi R}\frac{GM^2(r)}{r^3}. \tag{10}$$

The gas law,

$$P(r) = \frac{k}{\mu H}\rho(r)T(r). \tag{11}$$

2.3. Boundary conditions

Considering a sphere of infinitesimal radius r at the center, we find that $M(r) = 4\pi r^3\rho/3$. Since we may treat ρ sensibly constant in this sphere, then as $r\to0$, $M(r)\to0$, ρ remains finite as $r\to0$. It is also clear that $M(r) = M$ at the surface, i.e., at $r = R$. The protoplanets having cold origin must have a low surface temperature. In the first approximation we assume that the surface temperature is zero. The mass of the atmosphere of a protoplanet is just a minute fraction of its total mass, so we may take the pressure on its surface as approximately equal to zero. Therefore, the approximate boundary conditions can be given by

$$\left.\begin{array}{ll} T=0,\ P=0 & \text{at } r=R \\ M(r)=M & \text{at } r=R \\ M(r)=0 & \text{at } r=0 \end{array}\right\}. \tag{12}$$

3. Structure determination

3.1. Non-dimensionalisation

We have replaced the physical variables $P(r)$, $T(r)$, $M(r)$, and r by the non-dimensional variables p, t, q, and x respectively with the help of the following transformations

$$P(r)=\frac{GM^2}{4\pi R^4}p,\ T(r)=\frac{\mu HGM}{kR}t,\ M(r)=qM,\ \text{and } r=xR.$$

Here the symbol μ represents the mean molecular weight. By means of the above transformations and with the aid of the transformation $x = 1 - y$, Eqs. (8)–(10) with the help of Eq. (11), can be shown to be reduced to the form

$$\frac{dp}{dy}=\frac{pq}{t(1-y)^2}, \tag{13}$$

$$\frac{dq}{dy}=-\frac{p(1-y)^2}{t} \tag{14}$$

and $$\frac{dt}{dy}=C_R\frac{cpq^2}{(1-y)^3(at^4+bp)}, \tag{15}$$

as, by means of the above transformation, ρ is reduced to the form

$$\rho=\frac{M}{4\pi R^3}\frac{p}{t}. \tag{16}$$

In Eq. (15), $a=\frac{8\sigma H}{3\times10^{-24}}\left(\frac{\mu HGM}{kR}\right)^3$, $b=\frac{M\eta}{4\pi R^3}$, and $c=\frac{M^2k}{16\pi^2R^5\mu H}$.

The boundary conditions given by (12), then in terms of the non-dimensional variables can be written as

$$\left.\begin{array}{ll} t=0,\ p=0 & \text{at } y=0 \\ q(y)=1 & \text{at } y=0 \\ q(y)=0 & \text{at } y=1 \end{array}\right\}. \tag{17}$$

3.2. Numerical values used

A number of parameters are involved in our numerical calculations. The used values of masses and radii in our study are taken from the study of Helled and Schubert (2008). Besides those values, we take μ = 2.3 (Dullemond and Dominik, 2004), γ = 5/3 as is appropriate for a monoatomic gas and all other parameters involved have been assumed to have their standard values.

3.3. Numerical approach

It is evident that the Eqs. (13)–(15) as they stand cannot be solved analytically. Therefore, we must rely on the numerical method. However, because of the existence of vanishing denominators in the basic equations, integration cannot be started right from the surface or from the center. Therefore, we need to develop the solution near either of the boundaries and from this point with this development integrations can be started for varying y. The developed solution near the surface can be obtained by the standard method of series solution. Following Paul et al. (2008), they can be given by

$$p\approx a_0\frac{y^4}{(1-y)^4},\ t\approx\frac{c_0y}{(1-y)},\ q\approx1,\ \text{as } y\to0,\ \text{where } c_0 = 0.25 \text{ and } a_0=\frac{ac_o^5}{C_Rc-bc_0}.$$

With these values as our initial conditions, inserting values of the required parameters involved, we have solved Eqs. (13)–(15) numerically by the Classical fourth order Runge–Kutta

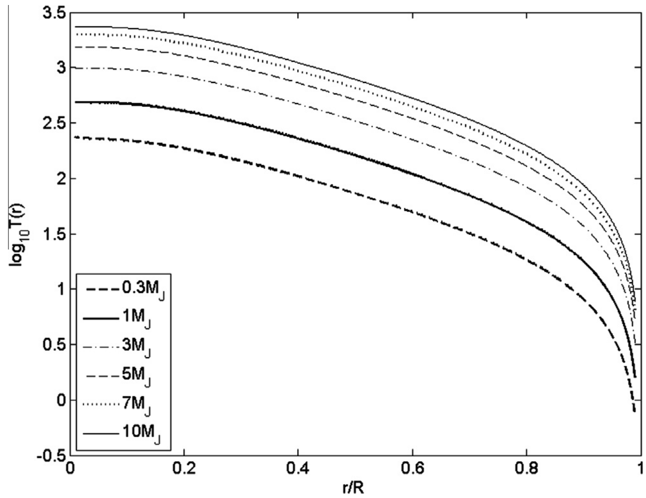

Figure 1 Temperature profiles inside some initial protoplanets. The dashed (thick), dotted, solid (thick), dashed (thin), solid(thin), dotted (thin) curves show the initial configuration for objects with 0.3, 1, 3, 5, 7 and 10 Jupiter masses respectively.

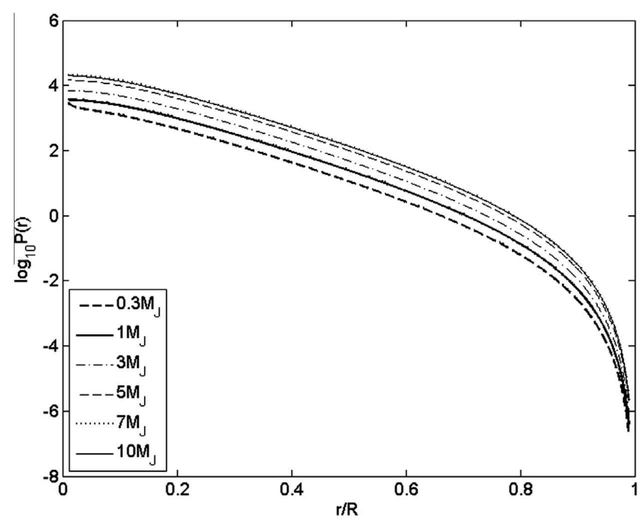

Figure 2 Pressure profiles inside some initial protoplanets. The dashed (thick), dotted, solid (thick), dashed (thin), solid(thin), dotted (thin) curves show the initial configuration for objects with 0.3, 1, 3, 5, 7 and 10 Jupiter masses respectively.

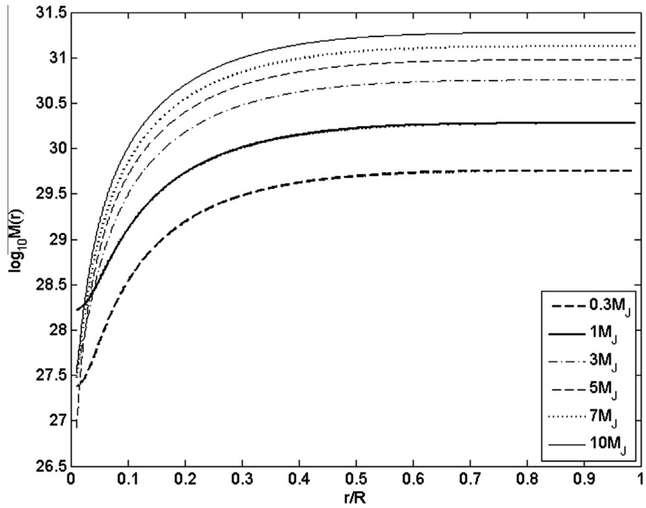

Figure 3 Mass distribution inside some initial protoplanets. The dashed (thick), dotted, solid (thick), dashed (thin), solid(thin), dotted (thin) curves show the initial configuration for objects with 0.3, 1, 3, 5, 7 and 10 Jupiter masses respectively.

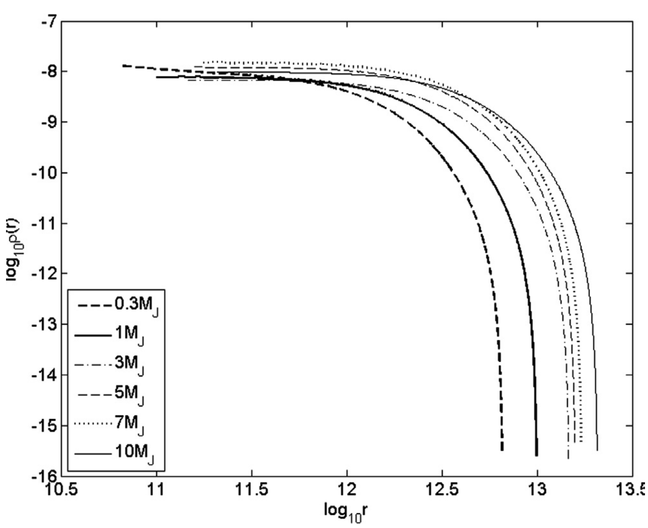

Figure 4 Density distribution inside some initial protoplanets. The dashed (thick), dotted, dashed-dotted, dashed (thin), solid (thin), and solid(thick) curves show the initial configuration for objects with 0.3, 1, 3, 5, 7 and 10 Jupiter masses respectively.

method from $y = 0.01$ downward to the point 0.999 to get the distribution of p, q, and t. The distribution of density is obtained using Eq. (16) with the determined distribution of p and t. The structures of the protoplanets are found to be dependent on a parameter C_R. The best values of C_R for the prescribed protoplanetary masses 0.3, 1, 3, 5, 7 and 10 M_J satisfying the third condition of (17) can be found to be 0.026, 0.2, 1.27, 2.43, 4.03 and 8.4 respectively. The results of our calculation are shown in diagrammatic forms through Figs. 1–4.

4. Result, discussion and conclusion

We have determined the distribution of thermodynamic variables inside protoplanets formed via disk instability in the mass range of 0.3–10 Jovian masses by the numerical method under approximate zero boundary conditions. The protoplanets have been assumed to be spheres of solar composition, each of which is in a steady state of quasi-static equilibrium in which the ideal gas law holds good, and the energy equation assumes the conduction–radiation heat transport. Fig. 1 depicts the temperature distribution inside some giant protoplanets with masses 0.3, 1, 3, 5, 7 and 10 Jupiter masses. It can be shown from the figure that the more massive is a protoplanet the hotter is its interior. The presented temperature profiles that come out through calculations are found to be in good agreement with the ones presented in Helled and Schubert (2008), Nayakshin (2010), Senthilkumar and Paul (2012). Fig. 2 shows our calculated pressure profiles inside the protoplanets with the assumed masses. It can be shown from the figure that after a point little depth from the surface down to the core region, the pressures of the protoplanets at a corresponding point increase with their increasing masses, except for the protoplanet with mass 10 M_J. Though the temperature profiles inside the assumed protoplanets predicted by the study can be found to be in good agreement with some previous investigations with more rigorous treatment of the problem our model can be found to predict objects with higher central pressure than the ones presented in Senthilkumar and Paul (2012) and Helled and Schubert (2008). It is to be noted here that Paul et al. (2012) and Senthilkumar and Paul (2012) assumed the initial protoplanets to be fully convective, while Helled and Schubert (2008) found such protoplanets to be fully convective with a thin outer radiative zone. Fig. 3 shows mass distribution inside the protoplanets considered. The figure shows that matter is not distributed uniformly in the atmosphere, and there may be variation in parameters due to gravitational stratification. This is to be expected for initial unsegregated protoplanets otherwise they could become so much centrally condensed. Fig. 4 depicts the distribution of density inside the protoplanets assumed. It can be observed from the figure that the surface density of the protoplanets with masses 0.3, 1, and 3 M_J decreases with decreasing mass but the central density of 3 M_J can be found to be higher than that of 1 M_J. On the other hand the protoplanet with mass 10 M_J can be found to be rarer in comparison with the protoplanets with masses 5 M_J and 7 M_J with respect to both central and surface densities. The density distribution obtained by the study is found to be consistent with the ones presented in Senthilkumar and Paul (2012). But Helled and Schubert showed that the surface density of such protoplanets decreases with their decreasing mass but the central density increases with their increasing mass. It is pertinent to point out here that initial configuration of the protoplanets formed via disk instability is still unknown and different numerical models predict different configurations (Helled and Schubert, 2008; Helled and Bodenheimer, 2011). However, the system possesses a unique solution which suggests that protoplanets formed via disk instability are a reasonable hypothesis. We have also tested our results for varying end points. The results are found to be insensitive to the choice of the end points. The results of our calculation may be important in the study of evolution of extrasolar giant planets. Future perspective of our research work concentrates on the evolution of extrasolar planets formed via disk instability based on the outputs obtained from this study.

References

Bohm-Vitense, E., 1997. In: Introduction to Stellar Astrophysics, vol. 3. Cambridge University Press.

Boley, A.C., Hartquist, T.W., Durisen, R.H., Michael, S., 2007a. The internal energy for molecular hydrogen in gravitationally unstable protoplanetary disks. Astrophys. J. 656, L89–L92.

Boley, A.C., Hartquist, T.W., Durisen, R.H., Michael, S., 2007b. Erratum: "the internal energy for molecular hydrogen in gravitationally unstable protoplanetary disks". Astrophys. J. 660, L175.

Boley, A.C., Hayfield, T., Mayer, L., Durisen, R.H., 2010. Clumps in the outer disk by disk instability: why they are initially gas giants and the legacy of disruption. Icarus 207, 509–516.

Boss, A.P., 1997. Giant planet formation by gravitational instability. Science 276, 1836–1839.

Boss, A.P., 2007. Testing disk instability models for giant planet formation. Astrophys. J. 661, L73–L76.

Cai, K., Durisen, R.H., Michael, S., Boley, A.C., Mejia, A.C., Pickett, M.K., D'Alessio, P., 2006a. The effects of metallicity and grain size on gravitational instabilities in protoplanetary disks. Astrophys. J. 636, L149–L152.

Cai, K., Durisen, R.H., Michael, S., Boley, A.C., Mejia, A.C., Pickett, M.K., D'Alessio, P., 2006b. Erratum: "the effects of metallicity and grain size on gravitational instabilities in protoplanetary disks". Astrophys. J. 642, L173.

Cha, S.-H., Nayakshin, S., 2011. A numerical simulation of a "super-Earth" core delivery from ∼100 to ∼8 AU. MNRAS 415, 3319–3334.

Dullemond, C.P., Dominik, C., 2004. The effect of dust settling on the appearance of protoplanetary disks. Astron. Astrophys. 421, 1075–1086.

Helled, R., Bodenheimer, P., 2011. The effects of metallicity and grain growth and settling on the early evolution of gaseous protoplanets. Icarus 211, 939–947.

Helled, R., Schubert, G., 2008. Core formation in giant gaseous protoplanets. Icarus 198, 156–162.

Hubickyj, O., Bodenheimer, P., Lissauer, J.J., 2005. Accretion of the gaseous envelope of Jupiter around a 5–10 Earth-mass core. Icarus 179, 415–431.

Mayer, L., Quinn, T., Wadsley, J., Stadel, J., 2002. Formation of giant planets by fragmentation of protoplanetary disks. Science 298, 1756–1759.

Mayer, L., Quinn, T., Wadsley, J., Stadel, J., 2004. The evolution of gravitationally unstable protoplanetary disks: fragmentation and possible giant planet formation. Astrophys. J. 609, 1045–1064.

Nayakshin, S., 2010. A new view on planet formation. arXiv:1012.1780.

Paul, G.C., Pramanik, J.N., Bhattacharjee, S.K., 2008. Structure of initial protoplanets. Int. J. Mod. Phys. A 23, 2801–2808.

Paul, G.C., Pramanik, J.N., Bhattacharjee, S.K., 2012. Gravitational settling time of solid grains in gaseous protoplanets. Acta Astronaut. 76, 95–98.

Pickett, B.K., Cassen, P., Durisen, R.H., Link, R., 2000. The effects of thermal energetics on three-dimensional hydrodynamic instabilities in massive protostellar disks. II. high-resolution and adiabatic evolutions. Astrophys. J. 529, 1034–1053.

Pollack, J.B., Hubickyj, O., Bodenheimer, P., Lissauer, J.J., Podolak, M., Greenweig, Y., 1996. Formation of the giant planets by concurrent accretion of solids and gas. Icarus 124, 62–85.

Senthilkumar, S., Paul, G.C., 2012. Application of new RKAHeM(4,4) technique to analyze the structure of initial extrasolar giant protoplanets. Earth Sci. Inf. 5, 23–31.